

GRB environment properties through X and Optical Afterglow observations

M.L. CONCIATORE⁽¹⁾, L.A. ANTONELLI⁽²⁾, G. STRATTA⁽³⁾, F. FIORE⁽²⁾
and R. PERNA⁽⁴⁾

⁽¹⁾ *Università degli Studi di Roma "La Sapienza", INAF-Osservatorio Astronomico di Roma*

⁽²⁾ *INAF-OAR*

⁽³⁾ *INAF-OAR & OMP*

⁽⁴⁾ *JILA-Boulder*

Summary. — We present the spectral analysis of 14 gamma-ray bursts (GRB) X-ray afterglows in order to investigate the properties of interstellar matter (ISM) along the line of sight of GRB. We carried out a simultaneous analysis of the NIR-optical and X-band for those afterglows with an optical counterpart too, in order to evaluate and strongly constrain the absorption effect on the spectral energy distribution due to dust extinction from GRB environment. We evaluated the equivalent hydrogen column density N_H from X-ray spectroscopy and rest frame visual extinction A_V by assuming different type of ISM composition and dust grain size distribution. From our analysis we obtained a distribution of the GRB rest frame consistent with the one expected if GRB were embedded in a Galactic-like molecular cloud. Moreover, values of the visual extinction estimated from the simultaneous analysis of NIR-to-X band favour an environment where small dust grain are destroyed by the interaction with the X-ray and UV photons from GRB.

PACS 98.70.Rz – gamma-ray sources; gamma-ray bursts.

PACS 98.58.Ca – Interstellar dust grains.

1. – Introduction

It's now generally believed that long-duration GRB are associated with the collapse of massive stars (e.g. [1]) and so a dense and dusty environment, typical of star forming regions, is expected in the nearby of the bursts. Up to now there are some observations that are in good agreement with this molecular cloud-like scenario, like the emitting and absorbing features observed in some X-ray afterglows (e.g. [2], [3]), the detection of a large amount of dust obtained from the high resolution spectroscopy of three optical afterglows [4] and the high rest frame visual extinction inferred in some other optical afterglows (e.g.[5]). Under this point of view, the non detection of $\sim 40\%$ of X-ray

TABLE I. – *X-ray afterglows sample.* ^aGalactic Coordinates (*J2000*), ^bRedshift, obtained through optical spectroscopy, ^cOptical Transient, ^dGalactic hydrogen column density along the line of sight of each GRB (from Dickey & Lockman maps [10])

GRB	^a <i>R.A.</i> (h m s)	^a <i>Dec</i> (° ’ ”)	^b <i>Z</i>	^c <i>OT</i>	^d N_H^{gal} ($10^{22} cm^{-2}$)
991216	05 09 31	+11 16 50	1.02	yes	0.27
000210	01 59 13	-40 40 46	0.846	no	0.0223
000926	17 04 10	+51 46 32	2.0375	yes	0.0265
001025	08 36 36.5	-13 04 30.3	1	no	0.065
011211	11 15 16.4	-21 55 44.8	2.14	yes	0.0427
020322	18 00 53.0	+81 04 48.0	1	no	0.045
020405	13 57 54	-31 23 34	0.691	yes	0.0427
020813	19 46 41	-19 36 00	1.254	yes	0.075
021004	00 26 54	+18 55 50	2.328	yes	0.0427
030226	11 33 03	+25 54 20	1.986	yes	0.0181
030227	04 57 29.0	20 29 23.9	1.6	yes	0.218
031203	08 02 30.0	-39 50 48.0	1	no	0.621
040106	11 58 50.5	-46 47 14.0	1	no	0.0842
040223	16 39 34.0	-41 55 45.0	1	no	0.663

afterglows at optical wavelengths (dark GRB) would be due to the dust absorption. On the other hand, the spectral energy distribution of some GRB afterglows indicates that dust reddening is very slow ([6],[7]). Moreover, for the observed optical afterglows, on average, the estimated rest frame visual extinction is a factor 10-100 lower than the expected if an ISM with dust to gas ratio and an extinction curve similar to the Galactic one are assumed ([8]). Also, some high redshift burst showed a larger amount of gas than dust. In a recent work, Stratta et al.([9]) already pointed out that absorption properties derived from X-ray and optical afterglows spectral analysis may require a “non-standard” extinction. A more careful study is required to probe the ISM of GRB environment.

In this work we present the results of a systematic multiwavelength spectra analysis of a sample of GRB afterglows in order to put some constraints on the properties of the circumburst environment.

2. – X-ray Data Analysis

We selected from the XMM-Newton and Chandra archives all the X-ray afterglows with an high signal-to-noise ratio (see Tab I) in order to perform a good spectral analysis. Standard data reduction in the 0.1-10.0 keV energy range was performed using SAS 6.0 for the data of the XMM-Newton EPIC instrument and using CIAO 2.3 for the Chandra ACIS-S instrument. All the spectra were analyzed with Xspec 11.2.0. In order to get Gaussian statistics, thus so to ensure the applicability of the χ^2 test to evaluate the goodness of our fits, the spectra were rebinned to obtain at least 20 counts per energy channel. For the EPIC spectra we performed simultaneous PN, MOS1 and MOS2 spectral fitting.

2.1. The spectral model. – According to the standard fireball model, the spectrum of the X-ray afterglows emission is well described by a simple power law $f_X(E) \propto E^{-\beta x}$. In this analysis we adopted a spectral model that takes into account also for the photoelectric absorption both Galactic and extragalactic due to the metal rich material along the line

of sight of GRB: $f_X \propto \left(E^{-\beta x} \times e^{-N_H^{gal}} \times e^{-N_H^Z} \right)$, where N_H^{gal} is the equivalent hydrogen Galactic column density fixed according to the Dickey & Lockman map [10] and N_H^Z is the extragalactic contribution to the absorption, whose value was left free to vary. The redshift values are derived from optical observation when available; otherwise, the value $z=1$ was adopted, being this the peak value of GRB redshift distribution[11].

2.2. Results. – We found an absorption larger than the Galactic value in nine cases (GRB000210, GRB001025, GRB020322, GRB020405, GRB020813, GRB030226, GRB030227, GRB031203, GRB040223) with confidence level up to 4σ . The rest frame equivalent hydrogen column density distribution obtained has a weighted average of $\langle N_H^Z \rangle = (1.0 \pm 0.1) \times 10^{22} \text{cm}^{-2}$, consistent with the theoretical peak expected if GRB are embedded in a Galactic-like molecular cloud (see Fig.1).

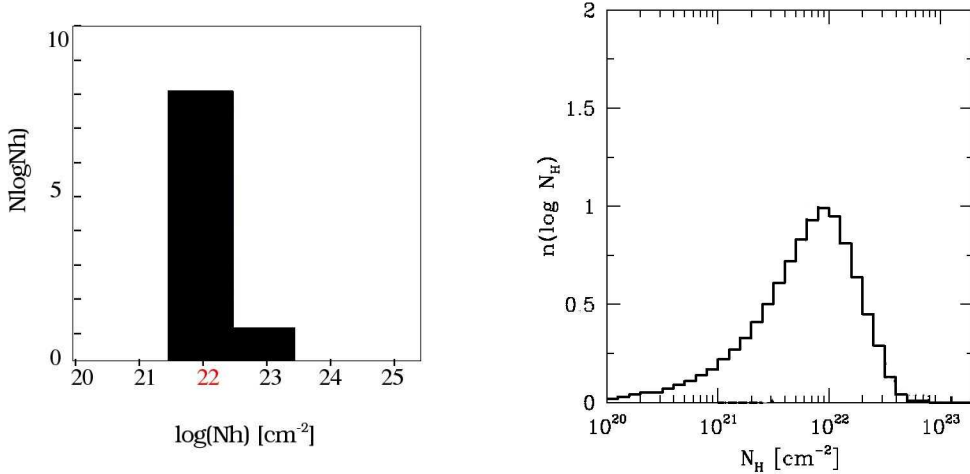


Fig. 1. – (Left) The rest frame equivalent N_H distribution obtained from the analysis in this work and the expected N_H^{Gal} distribution for GRB occurring in Galactic-like molecular cloud from Reichart & Price [12] (Right).

3. – Multiband analysis

For the eight afterglows of the sample with an optical counterpart (see TabI) the analysis was extended to the optical and NIR band, in order to better constrain extinction properties through a fit of spectra as wide as possible. Photometric data have been taken from literature. To perform this large band analysis we applied some correction to data. Firstly, being $F(t) \propto t^{-\alpha}$ we extrapolated magnitudes at the same time of X-ray observation, adopting the measured optical-NIR decay index published in literature and then we corrected them from Galactic extinction along GRB line of sight using the IRAS 100 $m\mu$ E(B-V) maps by Schlegel et al. 1998 [13] and by deriving the extinction at different wavelengths using the extinction curve parameterization taken from Cardelli et al. 1989 [14] assuming $R_V = A_V/E(B-V) = 3.1$. Finally, the magnitudes have been converted in fluxes using the effective wavelengths and normalization fluxes given by Fukugita et al. 1995 [15].

3.1. The spectral model. – For the optical/NIR data we adopted a model composed by a powerlaw and an absorption component that takes into account the dust extinction: $f_o(\lambda) = C\lambda^{-2-\beta}e^{(-A(\lambda r)/A_{Vr})A_{Vr}}$, where A_{Vr} is the visual extinction. Assuming the slow cooling regime as the most probable one for the electron population at the observation time, we assumed that the electron index p is twice the X-ray spectral index previously obtained within 90% confidence level. We fitted the data using both the possibility predicted for this regime: $\beta = (p - 1)/2$ if $\nu_{opt/NIR} < \nu_c$, $\beta = p/2$ if $\nu_{opt/NIR} > \nu_c$, where ν_c is the cooling frequency. We tested different dust composition and dust-to-gas ratio using different extinction curves, assuming that the dust grains distribution $n(a)$ is described by a simple power law $dn(a) \propto a^{-q}da$. The curves are: the Galactic-like (G) from Cardelli et al. 1989 [14], for which $q = -3.5$, $a_{min} = 0.005\mu m < a < a_{max} = 0.25\mu m$; the Small Magellanic Cloud-like (SMC) from Pei 1992 ([16]), that's the same model but with 1/8 of the solar metallicity; two extinction curves (Q1 and Q2) obtained by Maiolino et al 2000 ([17]), from simulation from study of a sample of AGN, for which $q = -3.5$, $a_{min} = 0.005\mu m < a < a_{max} = 10\mu m$ and $q = -2.5$, $a_{min} = 0.005\mu m < a < a_{max} = 1\mu m$ respective. We have also tested an extinction curve (C) derived by Calzetti et al. 2001 [18] for a sample of local starburst galaxies. For all this different ISM model the rest frame visual extinction has been estimated for all the afterglows sample.

3.2. Results. – For GRB991216 and GRB011211 we have obtained only the Galactic contribution to extinction, a result consistent with the previously X-ray analysis. For GRB000926, GRB020405, GRB020813, GRB030226 and GRB030227 the best fit is obtained assuming an ISM with dust grain distribution skewed toward large grains (Q1 curve for the first case, Q2 curve for the other four cases). We also compared the best fit additional N_H density at GRB's redshift with the best fit A_V obtained for the different extinction curves. The N_H/A_V relations have been compared with the corresponding theoretical one: Galactic, $N_H/A_V = 0.18 \times 10^{22} \text{ cm}^{-2}$ [8]; Small Magellanic Cloud, $N_H/A_V = 1.6 \times 10^{22} \text{ cm}^{-2}$ [19]; Q1, $N_H/A_V = 0.7 \times 10^{22} \text{ cm}^{-2}$ and Q2, $N_H/A_V = 0.3 \times 10^{22} \text{ cm}^{-2}$ [17]. For the starburst galaxies no N_H/A_V relationship has been derived due the complexity of this kind of ISM. Assuming a Galactic-like and SMC ISM, this ratio are well above the expected values, confirming previous studies (e.g. [7],[9]). A good agreement is obtained with an ISM with dust grain size distribution skewed toward large grain (see fig. 2). Such a dust composition reconciles the typical low reddening observed in the optical afterglows SEDs with the high amount of dust observed through optical spectroscopy [4]. This kind of environment can be obtained in two ways: small dust grain can coagulate into larger producing a dust distribution biased towards larger grains as expected in high density medium (e.g.[20]), or the physical state of the gas and dust are modified by the intense X-ray and UV emission from GRB, (e.g [21]).

Such an uncertainty will be solved by monitoring the very early afterglows and the possible evolution of the extinction effects. The SWIFT satellite and robotic telescopes, such as REM, will be very useful to provide us these informations.

* * *

For a more detailed analysis see Conciatore et al 2005 in prep.

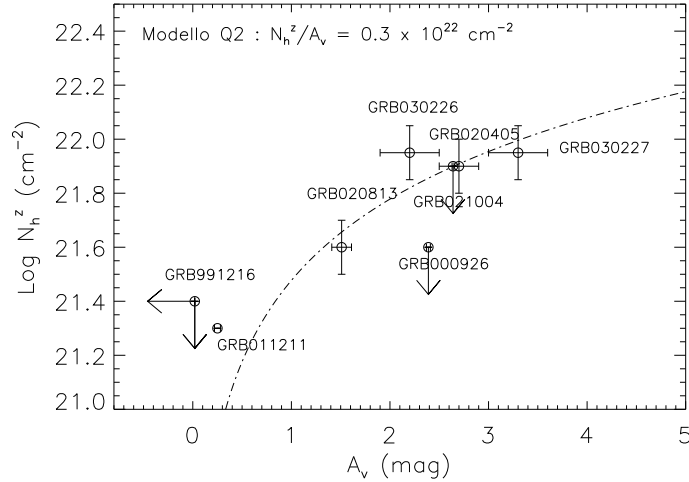


Fig. 2. – The best fit additional column density against best fit visual extinction obtained using Q2 curves.

REFERENCES

- [1] WOOSLEY S.E.; ZHANG W.; and HEGER A., *AIP Conference Proceedings*, **Vol 727** (2003)
- [2] ANTONELLI L.A. ET AL., *ApJ*, **545** (3) 2000
- [3] PIRO L. ET AL., *ApJL*, **514** (L73) 1999
- [4] SAVAGLIO S.; FALL M. and FIORE F., *ApJ*, **585** (638) 2003
- [5] BLOOM J.S.; DJORGOVSKI S.G. ET AL., *ApJ*, **507** (25B) 1998
- [6] SIMON V.; HUDEC R. ET AL., *A&A*, **377** (450) 2001
- [7] GALAMA T.J. and WIJERS R.A.M.J., *ApJL*, **549** (L209) 2001
- [8] PREDEHL P. and SCHMITT J.H.M.M., *A&A*, **293** (889) 1995
- [9] STRATTA G.; FIORE F.; ANTONELLI L.A.; PIRO L. and DE PASQUALE M., *ApJ*, **608** (864S) 2004
- [10] DICKEY J.M. and LOCKMAN F.J., *Ann. Rev. Ast. Astr.*, **28** (215) 1990
- [11] DJORGOVSKI S.G. ET AL., *proc. in Gamma-Ray Bursts in the Afterglow Era: 2nd Workshop*, edited by COSTA E.; FRONTERA F. and HJORTH J. (Berlin Heidelberg:Springer 2001, pp.218.
- [12] REICHART D.E. and PRICE P.A., *ApJ*, **565** (174) 2002
- [13] SCHLEGEL D.J.; FINKBEINER D.P. and DAVIS, M., *ApJ*, **500** (525) 1998
- [14] CARDELLI J.A.; CLAYTON G.C. and MATHIS, J.S., *ApJ*, **345** (245) 1989
- [15] FUKUGITA M.; SHIMASAKU K. and ICHIKAWA, T., *PASP*, **107** (945) 1995
- [16] PEI Y.C., *ApJ*, **395** (130) 1992
- [17] MAIOLINO A.; MARCONI A. and OLIVA E., *A&A*, **365** (37) 2001
- [18] CALZETTI D.; KINNEY A.L. and STORCHI-BERGMANN T., *ApJ*, **429** (582) 1994
- [19] WEINGARTNER J.C. and DRAINE B.T., *AAS*, **197** (4207) 2000
- [20] KIM S. and MARTIN P.G., *ApJ*, **462** (296K) 1996
- [21] WAXMAN E. and DRAINE B.T., *ApJ*, **537** (796) 2000